Plasmons in Scanning Transmission Electron Microscopy Electron Spectra

R. H. Ritchie
University of Tennessee

A. Howie
Cavendish Laboratory

P. M. Echenique
Universidad Pais Vasco

G. J. Basbas
Physical Review Letters

T. L. Ferrell
University of Tennessee

Recommended Citation

Ritchie, R. H.; Howie, A.; Echenique, P. M.; Basbas, G. J.; Ferrell, T. L.; and Ashley, J. C. (1990) "Plasmons in Scanning Transmission Electron Microscopy Electron Spectra," *Scanning Microscopy*: Vol. 1990 : No. 4 , Article 5.
Available at: https://digitalcommons.usu.edu/microscopy/vol1990/iss4/5

Utah State University
MERRILL-CAZIER LIBRARY

Plasmons in Scanning Transmission Electron Microscopy Electron Spectra

Authors

R. H. Ritchie, A. Howie, P. M. Echenique, G. J. Basbas, T. L. Ferrell, and J. C. Ashley

PLASMONS IN SCANNING TRANSMISSION ELECTRON MICROSCOPY ELECTRON SPECTRA

R. H. Ritchie,* A. Howie,[1] P. M. Echenique,[2] G. J. Basbas,[3]
T. L. Ferrell, and J. C. Ashley

Oak Ridge National Laboratory, P. O. Box 2008, Oak Ridge, TN 37831–6123 and
Department of Physics, University of Tennessee, Knoxville, TN 37996 USA
[1]Cavendish Laboratory, Madingley Road, Cambridge CB3 OHE, UK
[2]Universidad Pais Vasco, Facultad de Quimica, Aptdo 1072, San Sebastian, SPAIN
[3]Physical Review Letters, Box 1000, Ridge, New York 11961 USA

Abstract

A general self–energy formulation of the interaction between an electron in a scanning transmission electron microscope (STEM) and a localized target is given. We prove a theorem relating the probability of energy transfer to that calculated classically. Local dielectric theory of target excitation for various geometries is discussed. The problem of localization of initially unlocalized excitations in the valence band of solids is treated by transforming cross sections differential in momentum transfer into dependence on an impact parameter variable. We are thereby able to account for experimental data in scanning electron microscopy (SEM) that show high spatial resolution.

*Address for Correspondence:

R. H. Ritchie
Oak Ridge National Laboratory
Post Office Box 2008
Oak Ridge, TN 37831–6123
Telephone Number: (615) 574–6208

Introduction

Surface and bulk plasmon excitations in condensed matter by swift charged particles have been much studied for the last four decades [1–6]. Here we describe the excitation of such collective modes by swift electrons that may be formed into a beam incident on a localized target. Using the finely focused probe in the scanning transmission microscope (STEM), data can be collected with a spatial resolution of 2 nm or better in the region of surfaces, interfaces, small particles, and other features of inhomogeneous specimens. Energy analysis of the inelastically scattered electrons gives much useful information about the target. Such interactions involve the wave–particle duality of the electrons in an interesting context. We introduce a generalized self–energy formulation of the electron–target interaction that describes the full quantal properties of the probe. A general theorem relating the energy losses by an electron microprobe to those experienced by classical electrons with the same energy is described [7]. Recent progress in analyzing STEM data on energy losses in inhomogeneous targets using classical theory is reviewed. We also treat some aspects of secondary electron emission (SE) from such targets, emphasizing the localization of initially unlocalized excitations and the spatial distribution of collective modes created in the valence band of a solid.

The Self–Energy in STEM

It is convenient to use the self–energy concept in describing the interaction of a fast electron with an inhomogeneous target [8–13]. The essential quantal properties of the incident electron are properly treated, while the target is represented in terms of its response function. Information about the spatial dependence of the interaction probability may be inferred readily from the self–energy function. A general treatment of inelastic and elastic interactions in STEM has been given [14,15]. Here we use a different emphasis couched *a priori* in a mixed space–energy representation. This treatment is particularly appropriate to those interactions arising in STEM, where information about energy transfers to localized regions of space is of interest. Here we neglect relativistic effects and consider excitations of a target with characteristic energies $>>kT$, where T is the temperature of the target.

Consider the Green function $G_E(\mathbf{r},\mathbf{r}')$ describing the propagation of an electron with energy E from the

Figure 1

Figure 1. The Feynman diagram corresponding to the first–order self–energy of an electron interacting with a target as expressed in Eq. 2

(a)   Figure 2   (b)   (c)

Figure 2. Feynman diagrams representing higher–order contributions to the self–energy of an electron. Figure 2a corresponds to Eq. 5.

space point $\mathbf{r}$ to the point $\mathbf{r}'$. Many–body perturbation theory [16,17] may be invoked to write a Dyson integral equation for $G_E(\mathbf{r},\mathbf{r}')$ in terms of $G_E^0(\mathbf{r},\mathbf{r}')$, the noninteracting Green function;

$$G_E(\mathbf{r},\mathbf{r}') = G_E^0(\mathbf{r},\mathbf{r}')$$
$$+ \int d^3r_1 \int d^3r_2\, G_E(\mathbf{r},\mathbf{r}_2)\, \Sigma_E(\mathbf{r}_2,\mathbf{r}_1)\, G_E^0(\mathbf{r}_1,\mathbf{r}')\ . \tag{1}$$
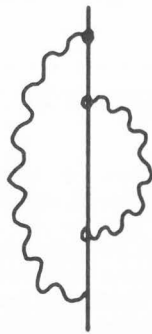
The spatially–dependent, proper self–energy, $\Sigma_E(\mathbf{r},\mathbf{r}')$, of the propagating electron due to interaction with the target, in turn may be expressed as an infinite series, the first term of which may be written

$$\Sigma_E^1(\mathbf{r},\mathbf{r}') = i\int \frac{dE'}{2\pi}\, G_{E-E'}(\mathbf{r},\mathbf{r}')\, W_{E'}(\mathbf{r},\mathbf{r}')\ . \tag{2}$$

The exact linear response function, or polarization propagator, for disturbances in the many–particle target is given by

$$W_E(\mathbf{r},\mathbf{r}') = \sum_n \left\{ \frac{\langle 0|\tilde{v}(\mathbf{r})|n\rangle \langle n|\tilde{v}(\mathbf{r}')|0\rangle}{\mathscr{E}_{0n} + E + i\alpha} \right.$$

$$\left. + \frac{\langle 0|\tilde{v}(\mathbf{r}')|n\rangle \langle n|\tilde{v}(\mathbf{r})|0\rangle}{\mathscr{E}_{0n} - E + i\alpha} \right\}\ , \tag{3}$$

where α is a positive infinitesimal, $(|0\rangle,\ |n\rangle)$ is the exact state vector of the many–particle target in the (ground, nth excited) state and $\mathscr{E}_{0n} = \mathscr{E}_0 - \mathscr{E}_n$, where $(\mathscr{E}_0,\ \mathscr{E}_n)$ is the energy of the (ground, nth excited) state. The interaction energy $\tilde{v}(\mathbf{r})$ may be expressed in terms of $(\hat{\Psi}^+(\mathbf{r}),\ \hat{\Psi}(\mathbf{r}))$, the wave (creation, annihilation) operator for a particle at position $\mathbf{r}$ in the target, viz.,

$$\tilde{v}(\mathbf{r}) = e^2\int d^3r'\, \frac{\hat{\Psi}^+(\mathbf{r}')\, \hat{\Psi}(\mathbf{r}')}{|\mathbf{r} - \mathbf{r}'|}\ , \tag{4}$$

for Coulomb interactions between electrons in the target. We neglect elastic scattering for the present purposes. The Feynman diagram of Fig. 1 illustrates the interaction corresponding to Eq. 2.

A term of next higher order in the electron–target interaction may be written,

$$\Sigma_E^{2a}(\mathbf{r},\mathbf{r}') = -\int \frac{dE_1}{2\pi} \int \frac{dE_2}{2\pi} \int d^3r_1 \int d^3r_2\, G_{E-E_1}(\mathbf{r},\mathbf{r}_2)$$
$$\times\, W_{E_1}(\mathbf{r},\mathbf{r}')\, G_{E-E_1-E_2}(\mathbf{r}_2,\mathbf{r}_1)$$
$$\times\, W_{E_2}(\mathbf{r}_2,\mathbf{r}_1)\, G_{E-E_1}(\mathbf{r}_1,\mathbf{r}')\ , \tag{5}$$

corresponding to the Feynman diagram of Fig 2a. Figures 2b and 2c illustrate two other contributions to Σ_E of this same order. Note that the self–energy diagram of Fig. 2c is obtained if we replace G by G^0 in Eqs. 2 and 5. It does not correspond to the "proper" self–energy, found algebraically in a straightforward manner for translationally invariant systems, and discussed in the literature (see Refs. 10,11). Generalization to still higher–order terms is straightforward [11,12].

Analytical solution of the Dyson equation (Eq. 1 above) is not possible for systems without translational invariance. Here we approximate the self–energy of a projectile interacting with an arbitrary target by a series of terms that are ordered according to the number of times the projectile interacts with the target. In doing so we use the linear response function of the target since we expect that this procedure will yield reasonable results in many cases.

The electron Green function may be approximated in the standard form

$$G_E(\mathbf{r},\mathbf{r}') = \sum_k \frac{u_k(\mathbf{r})\, u_k^*(\mathbf{r}')}{E - E_k + i\delta}\ , \tag{6}$$

46

where $u_k(r)$ is an exact eigenfunction for the fully interacting electron, E_k is the eigenenergy of this state and δ is a positive infinitesimal.

If the electron is prepared in a state specified by the state function $\psi_0(r)$, then the "averaged" self–energy

$$\Sigma_0 = \int d^3r \int d^3r' \ \psi_0(r) \ \Sigma_{E_0}(r,r') \ \psi_0^*(r') \qquad (7)$$

is complex. Its real part yields the shift in the electron's energy while the imaginary part, when multiplied by $2/\hbar$, gives the rate at which it is scattered out of the initial state. E_0 is understood here to be the energy of the state corresponding to ψ_0.

Equation 7 may be simplified by using Eq. 6 for $G_E(r,r')$ and by approximating the exact $\Sigma_E(r,r')$ by its lowest–order form $\Sigma_E^1(r,r')$ from Eq.2. Then

$$\Sigma_0^1 = \sum_k \int \frac{i dE'}{2\pi} \int d^3r \int d^3r'$$

$$\times \frac{\psi_0^*(r) \ u_k(r) u_k^*(r') \ \psi_0(r')}{E_0 - E_k - E' + i\delta} \ W_{E'}(r,r') \quad . \qquad (8)$$

This is a generalization of an expression given in [11] for Σ_0^1. Using the Lehmann form, Eq.3, for W,

$$\Sigma_0^1 = \sum_k \sum_n \int d^3r \int d^3r' \ \frac{\psi_0^*(r) u_k(r) u_k^*(r') \psi_0(r')}{E_{ok} + \epsilon_{on} + i\delta}$$

$$\times \langle o|\tilde{v}(r)|n \rangle \ \langle n|\tilde{v}(r')|o \rangle \quad . \qquad (9)$$

Excitation of a Target by a Microprobe

Consider the excitation of a localized target situated near the origin of coordinates by an electron prepared in the form of a narrow beam. Figure 3 shows a schematic representation of such a STEM configuration. Represent the electron by the wave packet [7]

$$\psi_0(r) = \int \frac{d^2Q}{(2\pi)^2} \ \phi_Q \ \exp\left[iQ\cdot(\rho - b)\right]$$

$$\times \exp\left[iz(k_0^2 - Q^2)^{1/2}\right] / L^{1/2} \quad , \qquad (10)$$

where ϕ_Q is chosen so that at $z=0$ the packet is distributed in a narrow probe about the impact parameter b with spatial extension $\sim\Delta$ about b. The factor in the wave function describing the z–variation is normalized in the large spatial interval of length L. The self–energy of this electron may be evaluated in a
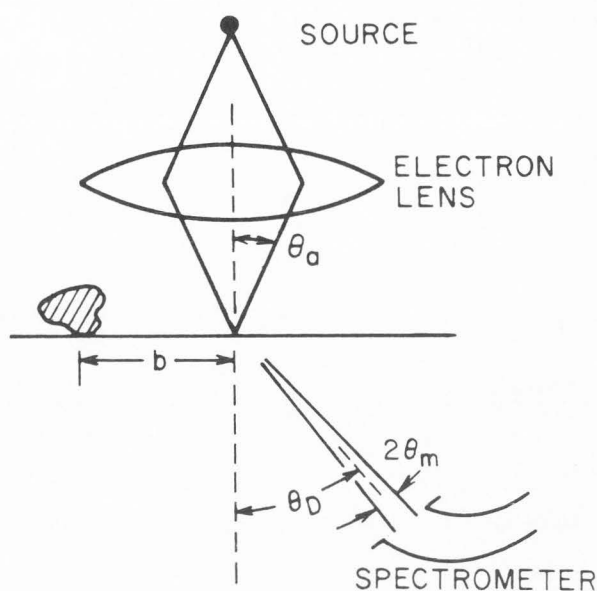

Figure 3. A schematic diagram representing a typical STEM configuration. The target is located at impact parameter b with respect to the focused beam and the energy analyzer subtends the half–angle θ_m at the angle θ_D with respect to the incident beam.

straightforward way from Eq. 7 in lowest order when one takes

$$G_E(r,r') \approx G_E^0(r,r') =$$

$$\sum_k \frac{\exp[i k \cdot (r-r')]/L^3}{[E - E_k + i\delta]} \quad . \qquad (11)$$

One finds after evaluating the integral over E' in Eq. 8 by contour integration

$$\Sigma_0^1 = \sum_k \sum_n \int d^3r \psi_0^*(r) \int d^3r' \psi_0(r')$$

$$\times \frac{\langle o|\tilde{v}(r)|n \rangle \ \langle n|\tilde{v}(r')|o \rangle}{E_0 - \epsilon_{no} - E_k + i\delta} \frac{\exp\left[i k \cdot (r-r')\right]}{L^3} \qquad (12)$$

Multiplying Im Σ_0^1 by $2/v$, where $v = \hbar k_0/m$, summing over all final states of the electron and singling out a particular state $|n \rangle$ of the target, one may show [7] that P_n^q, the resulting probability of exciting the nth state in transitions of the electron to all possible plane wave final states, is

$$P_n^q = \int d^2\rho \ | \ \phi(\rho - b) \ |^2 P_n^c(\rho) \quad . \qquad (13)$$

47

In obtaining this result one assumes that $k_0 >> Q$ for values of Q for which ϕ_Q is not much smaller than unity, and that recoil corrections to the final energy due to momentum transfers perpendicular to the beam direction may be neglected. This is described in more detail in [7].

Here $P_n^{\ c}(\rho)$ is the probability of exciting the target by a classical electron with the same velocity at impact parameter ρ and $|\phi(\rho-b)|^2$ is the probability of finding the electron at that impact parameter. Also, $\phi(\rho) = \int d^2Q \exp(iQ\cdot\rho)\phi_Q/(2\pi)^2$. This quite general result shows that, if all inelastically scattered electrons are collected by the energy analyzer, the measured probability of exciting a given transition may be computed theoretically as if the beam consisted of a superposition of classical trajectories distributed laterally to the beam direction according to the probability density $|\phi(\rho-b)|^2$. Saying this another way, provided that the spectrometer aperture in the STEM is large enough to accept most of the inelastic scattering, classical excitation functions are correct when averaged over a range of impact parameters corresponding to the current distribution in the probe. In [7] partial signal collection is considered in detail. The probability of surface plasmon generation at a planar surface by a probe and with collection of scattered electrons by a small spectrometer aperture placed at various angles is evaluated numerically. With off–axis positions improved spatial resolution is obtained. In all detector positions the width of the microprobe emerges from the wave theory as an obvious limit to the obtainable resolution.

The Self–Energy of an Aloof Probe Exciting Surface Modes

Consider an electron prepared in a state corresponding to the wave packet of Eq. 10 and traveling parallel with and at distance x from a condensed matter surface. Assuming that $k_0 >> Q$ in Eq. 10 and using the approximation of Eq. 11, one finds

$$\Sigma_0^1 = \sum_{k_z} \sum_{k_\rho} \int \frac{idE'}{2\pi} \int d^3r \int d^3r' \ \phi^*(\rho-b)$$

$$\times \frac{\exp(-i\,zk_0)\ \exp(ik\cdot[r-r'])\ \exp(iz'k_0)}{L^4\left[\frac{\hbar^2}{2m}(k_0^{\ 2}-k_\rho^{\ 2}-k_z^{\ 2})-E'+i\delta\right]}$$

$$\times \phi(\rho'-b)\ W_E{}'(r,r')\quad. \tag{14}$$

where $k = (k_\rho, k_z) = (k_x, k_y, k_z)$. $W_E(r,r')$, the propagator for disturbances in the medium, may be evaluated in various approximations. For a metal, one might use the specular reflection model [18], or a hydrodynamical model [4,19]. For simplicity we use a local dielectric model, in which case

$$W_E(r,r') = \int \frac{d^2\kappa}{(2\pi)^2}\frac{2\pi e^2}{\kappa}\left[\frac{1-\epsilon_\omega}{1+\epsilon_\omega}\right]\exp\left[i\kappa\cdot(R-R')\right]$$

$$\times \exp\left[-\kappa(x+x')\right] \tag{15}$$

Here $R=(0,y,z)$, $\kappa=(0,\kappa_y,\kappa_z)$, $\omega=E/\hbar$ and it is understood that ϵ_ω is a time–ordered local dielectric function, such that $\epsilon_\omega=\epsilon_{-\omega}.$[1] We also assume that the probe does not penetrate into the solid, although it is straightforward to write down a formula for $W_E(r,r')$ that accounts for this possibility [13].

Neglecting $k_\rho^{\ 2}$ in the denominator of Eq. 14, summing over all k_ρ and defining a projected, or local, self–energy, $\Sigma_0^1(x)$, as [11]

$$\Sigma_0^1 = \int dx \int dy\ \phi^*(\rho)\ \Sigma_0^1(x)\ \phi(\rho)\quad, \tag{16}$$

where $\rho=(x,y,0)$, one finds after equating integrands,

$$\Sigma_0^1(x) = \int \frac{idE'}{2\pi} \int \frac{d\kappa_z}{2\pi} \int \frac{d\kappa_y}{2\pi}$$

$$\times \frac{\frac{2\pi e^2}{\kappa}\left[\frac{1-\epsilon_{\omega'}}{1+\epsilon_{\omega'}}\right]\exp(-2\kappa x)}{[\hbar v\kappa_z - E' + i\delta]}\quad. \tag{17}$$

The neglect here of a term $k_z^{\ 2}/2$ in the denominator should be quite accurate for the high–energy electrons used in STEM. The imaginary part of Eq. 17 may be expressed simply by using Dirac's formula for the denominator, i.e., $1/(\omega+i\alpha)=P/\omega-i\pi\delta(\omega)$, where $\delta(\omega)$ is the Dirac delta function, one finds

$$Im\ \Sigma_0^1(x) = \frac{e^2}{\pi v}\int_0^\infty d\omega\ K_0(\frac{2\omega x}{v})\ Im\left[\frac{1-\epsilon_\omega}{1+\epsilon_\omega}\right]\quad, \tag{18}$$

where K_0 is the modified Bessel function of the second kind. If we use the electron gas model, $(1-\epsilon)/(1+\epsilon)=\omega_s^2/[\omega^2-(\omega_s-i\alpha)^2]$ where $\hbar\omega_s$ is the surface plasmon energy and α is a positive infinitesimal. Then

---

[1]The time-ordered dielectric function has zeros in the second and fourth quadrants of the complex ω-plane such that $\epsilon_\omega = \epsilon_{-\omega}$. The causal ϵ_ω^c, familiar from classical dielectric theory, has zeros lying in the third and fourth quadrants, such that $\epsilon_\omega^c = (\epsilon_{-\omega}^c)^*$. It is straightforward to construct the time-ordered ϵ from the causal ϵ^c, given the latter either from experiment or in analytical form.

evaluating the integral of Eq. 17 over E′ by contour integration methods, one finds

$$\text{Re } \Sigma_0^1(x) = -\frac{e^2 \omega_s}{2v} \int_0^{\pi/2} d\theta \, \exp(-2\omega_s x \sin\theta/v) \quad , (19)$$

which goes asymptotically, as x→∞, to the form $\text{Re}\Sigma_0^1 = -e^2/4x$, the classical image potential for an electron at distance x from a perfect conductor [11,20]. One obtains also [21]

$$\text{Im } \Sigma_0^1(x) = -\frac{e^2 \omega_s}{2v} K_0 \left[\frac{2\omega_s x}{v} \right] \quad . \quad (20)$$

In the approximation leading to Eq. 17, $\Sigma(x)$ does not depend at all on the form of the microprobe. In general, and in a more detailed treatment [11,22], one finds such a dependence.

Higher–order terms in the self–energy function have been worked out for slow electrons near a metal surface [12].

The form of $W_E(\mathbf{r}, \mathbf{r}')$ for a spherical target characterized by a local dielectric function has been given in [13] and employed to evaluate Im Σ and the closely related quantity P_ω, the differential probability for losing energy $\hbar\omega$ to the target.

Classical Dielectric Theory of Excitation

Interest in the use of the low–loss, valence excitation region of the spectrum has been recently revived after having been dormant for several years. For example, one can study surface excitation generated when a beam is outside the sample as in reflection electron microscopy (REM) imaging or in the so–called aloof beam [23] studies [24–26] of small particles. Localized, low–loss electron spectroscopy in inhomogeneous samples is reemerging as a potentially important new adjunct of electron microscopy.

In view of the demonstration above and in Ref. [7] that a classical treatment of energy losses is valid when the energy loss spectrometer collects most of the scattered angular distribution, it is of some interest to review work on the local dielectric treatment of the interaction of electrons, assumed to move on classical trajectories, with various targets.

A Classical Electron Moving Parallel with a Plane-Bounded Dielectric

One may compute the retarding field, and hence the rate of energy loss experienced by a fast electron traveling parallel with, and at distance from, a surface using ordinary local dielectric theory. One finds for the probability of exciting the dielectric per unit path length,[2]

$$\frac{dP(x)}{dz} = \frac{2e^2}{\pi\hbar v^2} \int_0^\infty d\omega \, K_0\left(\frac{2\omega x}{v}\right) \text{Im}\left(\frac{1-\epsilon}{1+\epsilon}\right) \quad , (21)$$

---

[2]Ritchie RH (1982). Quoted in Ref. [25].

when the trajectory lies outside of the dielectric and in a medium with unit dielectric constant. This result is identical with that found in the wave treatment above in Eq. 18 after multiplying Eq. 18 by 2 to go from a probability amplitude to a probability, dividing by $\hbar$ to obtain a damping rate and then further dividing by v to get a probability per unit path length.

When x<0 and the electron travels in the dielectric,

$$\frac{dP(x)}{dz} = \frac{2e^2}{\pi\hbar v^2} \int_0^\infty d\omega \left[\text{Im}(\frac{-1}{\epsilon}) \left\{ \ln \frac{q_c v}{\omega} \right. \right.$$
$$\left. \left. -K_0\left[\frac{2\omega|x|}{v}\right] \right\} + \text{Im}\left[\frac{1-\epsilon}{1+\epsilon}\right] K_0\left[\frac{2\omega|x|}{v}\right] \right] \quad . \quad (22)$$

The term containing the factor $\text{Im}(-1/\epsilon)$ describes losses to bulk modes. The logarithmic term yields the ordinary loss rate to volume excitations, q_c is a cutoff wave number, and the K_0 function describes the boundary (or "begrenzung") correction to these losses [4].

Here ϵ_ω is either the time–ordered or causal dielectric function of the target, and $\omega = \Delta E/\hbar$, where ΔE is the energy loss. In case the region x>0 is filled, instead, with material having dielectric function ϵ_ω^0, one needs only replace the factor $\text{Im}[(1-\epsilon)/(1+\epsilon)]$ by $\text{Im}[(\epsilon^0-\epsilon)/(\epsilon^0+\epsilon)]$ to account for the altered surface excitation function and employ a factor like the bulk response function of Eq. 22 in the region x>0 but with $\text{Im}(-1/\epsilon)$ replaced by $\text{Im}(-1/\epsilon^0)$.

Equation 21 may be modified [24] to deal with the case of a beam reflecting from a surface at a small glancing angle by putting $dz=dx/\theta$ and integrating over x. This gives the total probability of surface excitation in such a trajectory, counting both incoming and outgoing segments, as

$$P(\theta) = \frac{e^2}{\hbar v \theta} \int_0^\infty \frac{d\omega}{\omega} \text{Im}\left[\frac{1-\epsilon}{1+\epsilon}\right] \quad (23)$$

Comparing experimental data on loss spectra using Cu surfaces with the function $\text{Im}[(1-\epsilon)/(1+\epsilon)]/\omega$, Howie and Milne [27] found reasonable agreement between them despite the presence of an oxide layer.

Generalization of Eqs. 21–23 to take account of relativistic effects has been made in [28]. However, the relativistic corrections are expected to be small unless $\text{Re}(\epsilon)$ becomes large enough that the criterion for the emission of Cherenkov photons ($\epsilon v^2/c^2 > 1$) is satisfied for an appreciable range of frequencies.

One notes that the function $K_0(2\omega x/v)$ diverges logarithmically as x → 0 and that Eqs. 21–22 must lose validity in that limit. Echenique [29] has evaluated the error incurred in using a local ϵ and finds that for x<1 nm appreciable errors may be expected at typical STEM conditions.

Milne and Echenique [30] have compared the predictions of surface plasmon excitation calculated from Eq. 21 with STEM data taken on MgO cubes. They evaluate the probability of excitation as a function of the distance from the face of a cube and find good agreement
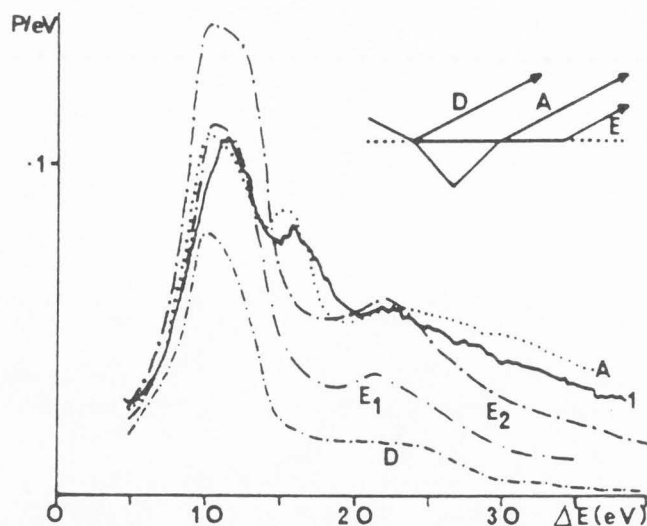
Figure 4. Experimental specular beam energy loss spectrum [49] obtained at the 880 diffraction conditions in GaAs with 100 keV electrons. The broken curves are computed for a trajectory A with exponential depth penetration (decay depth = 3.3 nm), for a trajectory D reflecting at the surface and for trajectories traveling along the surface for 82 nm (E_1) and for 120 nm (E_2) as shown in the inset.

if they use experimentally determined ϵ_ω values. For $x \gtrsim 10$ nm the use of relativistic corrections yields better agreement than when the nonrelativistic formula Eq. 21 is used.

In several papers [27,31–34], workers at the Cavendish Laboratory have analyzed data taken in Reflection High Energy Electron Diffraction (RHEED) and Reflection Electron Microscopy (REM). They treated grazing trajectories as a series of short segments parallel to the interface and at different distances from it and have included relativistic and finite aperture effects as well as some penetration of the crystal before reflection. They find that simple dielectric theory seems to allow fitting of the data in absolute terms. Figure 4 shows typical reflection energy loss spectra [32] obtained with a GaAs surface as compared with calculations using dielectric theory. They have also developed a quasi–planar approximation to the excitation of geometrically complex dielectrics [32].

Excitation of Dielectrics in Other Geometries

Analytical solutions have been obtained for the excitation produced by a fast classical electron passing near a spherical dielectric body. When the electron passes at distance b from the center of a sphere of radius a<b, the excitation probability per unit energy range is given by [35,36]

$$\frac{dP}{\hbar d\omega} = \left[\frac{4e^2a}{\pi\hbar^2 v^2}\right] \sum_{\ell=0}^{\infty} \sum_{m=0}^{\ell} \frac{2-\delta_{om}}{(\ell-m)!\,(\ell+m)!}$$

$$\mathrm{Im}(-\gamma_\ell(\omega))\,\left(\frac{\omega a}{v}\right)^{2\ell} K_m^{\ 2}\left(\frac{2\omega b}{v}\right) \quad , \qquad (24)$$

where

$$\gamma_\ell(\omega) = \frac{1-\epsilon_\omega}{1+\epsilon_\omega+\ell^{-1}} \quad .$$

The nonrelativistic theory leading to Eq.24 has been extended to oxide–coated spheres [36] as well as to the case where the trajectory passes through the sphere [13]. The results are in qualitative agreement with experiment [36–39], but more work is needed here.

Excitation functions for dielectric bodies bounded by more elaborate coordinate systems have been found. These include some allowance for the effect of the support of a spherical particle [38,39] and for interactions between closely–spaced pairs of spherical particles [40,41]. A spheroidal dielectric has been studied [42]. Solutions found for a cylindrical wedge [43,44] have relevance to the case of a fast electron passing near a corner of a cube.

Results for excitation of a dielectric by a fast electron passing through a cylindrical cavity in the medium have also been obtained [45–47]. It has been possible to interpret in considerable detail [47] the energy loss spectra obtained experimentally in this geometry.

Spatial Resolution in Energy Loss Spectroscopy

An estimate of the effective distance from the track of a swift electron at which excitation of an electronic transition with energy transfer $\hbar\omega$ will occur can be made on the basis of the duration of the electric impulse experienced at a given impact parameter by a struck electron. This yields the "cutoff" impact parameter $b_c = v/\omega$. For a 15 eV-loss with 100-keV electrons this comes to ~7 nm.

Cheng [48] has pointed out that this figure is considerably larger than the spatial resolution of 0.4 nm that has been achieved in some experiments [49] using the 15-eV loss in Al. He identifies the resolution found with the distance traveled by the plasmon before it decays and gets quantitative agreement between his theory and experiment using reasonable estimates of the plasmon group velocity and lifetime. In our view, this explanation is suspect. It is important to realize that b_c is an upper estimate of the impact parameter corresponding to zero scattering angle and thus zero momentum transfer perpendicular to the initial velocity. Larger values of momentum transfer are associated with smaller interaction distances. The strength of the excitation at a given energy loss is in general determined by an integral over momentum transfer and ultimately depends on some function of $\omega b/v$, such as the function $K_0(2\omega b/v)$ in the case of a planar interface (Eq. 20 above) or the function $K_0^2(\omega b/v) + K_1^2(\omega b/v)$, which is appropriate in the dipole limit for a very small sphere. Recent success [50] in the high spatial resolution band gap spectroscopy of defects in semiconductors lends some support to the latter expression. The function $K_0(\omega b/v)$ varies quite rapidly with $\omega b/v$ as its argument increases, particularly in the interval $\omega b/v < 1$. Thus we suggest that the observed high spatial resolution in [49] may be due to the relatively large momentum components

available in the excitation spectrum of the plasmon.[3] This point is discussed below in connection with secondary electron emission in SEM.

Secondary Electron Generation Processes and their Degree of Localization

The secondary electron (SE) signal has long been recognized in scanning electron microscopy as the most useful indicator of surface topography. Recent work in STEM [51,52] has shown that it is possible to obtain SE signals with 1-nm spatial resolution and 1-eV energy resolution and that reflection SE images of oxidized Cu show oxide islands and details of their interaction with surface steps. The generation of secondary electrons by fast incident electrons is quite complex, involving electron cascade processes created by fast secondaries and the slowing–down of the resulting knock-ons as well as the decay of inner-shell vacancies and collective states in the valence band. The relative importance of these different excitation processes has been considered by a number of authors but less attention has been paid to assessing their degree of localization, i.e., the relevant impact parameter or distance from the electron beam where the secondary is generated.

Elaborate calculations have been made for Al [53,56] indicating that plasmon excitation followed by decay into electron–hole pairs makes the dominant contribution to the SE signal. Monte Carlo calculations by Luo and Joy [57] show that the majority of secondaries originate from plasmon decay. Others [51,52] question whether plasmon decay is sufficiently well–localized to explain their measured high spatial resolution.

To extract a spatial representation from the quantal expression for the probability of energy transfer to a condensed medium from a swift charged particle, we have considered three alternative formulations [58,59] that we now describe.

The Impact Parameter Representation (IPR)

The problem of visualizing quantal collisions in the space (and perhaps time) variable has been faced by several workers over the years [60–63]. The lack of a comprehensive theory of an impact parameter representation for collisions in condensed matter has been noted long ago [63]. We approach this problem by using an expression for the probability of interaction of a fast electron with a medium whose response is specified in terms of a dielectric function $\epsilon_{k,\omega}$ that depends on energy transfer, $\hbar\omega$, and the magnitude of the momentum transfer, $\hbar k$, to the medium. A more general formulation in terms of the dielectric matrix of the medium is possible but we have not yet done this. We write for the differential inverse mean free path (DIMFP) for energy and momentum transfer to the medium by the electron

$$\frac{d^3\Lambda^{-1}}{d\omega d^2\kappa} = \frac{e^2}{\pi^2\hbar v^2}\frac{1}{k^2}\text{Im}\left[\frac{-1}{\epsilon_{k,\omega}}\right] \quad , \qquad (26)$$

---

[3]Theoretical determinations of the probability of excitation of a surface plasmon by a STEM electron as a function of distance from a planar dielectric are being carried out by Zabala and Echenique. These account for plasmon damping and dispersion and still show good spatial resolution.

where $\hbar\kappa$ is the momentum transfer perpendicular to the electron direction. The magnitude of the total momentum $\hbar k = \hbar(\kappa^2 + \omega^2/v^2)^{1/2}$.

The Chang–Raman Transform

In the context of theoretical high energy physics, Chang and Raman [64] have employed a mathematical transformation from momentum to a space–like variable. It has been advocated for use in radiation physics [63]. Following their lead one transforms variables from κ to impact parameter b. This may be done by first integrating Eq. 26 over ω to obtain

$$\frac{d^2\Lambda^{-1}}{d^2\kappa} = \frac{e^2}{\pi^2\hbar v^2}\int_0^\infty \frac{d\omega}{k^2}\text{Im}\left[\frac{-1}{\epsilon_{k,\omega}}\right] \equiv \left|\sigma(\kappa)\right|^2$$

where the second equality is allowed because $\text{Im}(\frac{-1}{\epsilon})$ is a positive definite quantity. We now seek to eliminate κ in favor of a spatial variable that will be interpreted as an impact parameter. Thus

$$\Lambda^{-1} = \int d^2\kappa \left|\sigma_\kappa\right|^2 = \int d^2\kappa \int d^2\kappa'\, \sigma(\kappa)\sigma^*(\kappa')$$

$$\times\, \delta^2(\kappa-\kappa')$$

$$= \frac{1}{(2\pi)^2}\int d^2\kappa \int d^2\kappa'\, \sigma(\kappa)\sigma^*(\kappa')\int d^2b\, \exp(ib\cdot[\kappa-\kappa'])$$

$$= \frac{1}{(2\pi)^2}\int d^2b \left|\int d^2\kappa\, \exp(i\kappa\cdot b)\, \sigma(\kappa)\right|^2$$

The integrand of this equation is now set equal to the DIMFP in impact parameter space, viz.,

$$\frac{d^2\Lambda_{CR}^{-1}}{d^2b} = \frac{e^2}{4\pi^4\hbar v^2}\left|\int d^2\kappa\, \exp(i\kappa\cdot b)\right.$$

$$\times\left.\left\{\int_0^\infty \frac{d\omega}{k^2}\text{Im}\left(\frac{1}{\epsilon_{k,\omega}}\right)\right\}^{1/2}\right|^2 \, . \qquad (27)$$

One may easily apply this to analytical forms for $\epsilon_{k,\omega}$ of an electron gas. However, for reasons given elsewhere [65], the transformed function described next is preferable to that found using the Chang–Raman method.

The Energy–Transfer Transform

We have made a more general approach [65] by employing a transform different from, but related to, that of Chang and Raman. We write

$$\frac{d\Lambda^{-1}}{d\omega} = \frac{1}{\hbar}\left[\frac{e}{2\pi^2 v}\right]^2\int d^2b \int d^2\kappa \int d^2\kappa'$$

$$\exp[2b\cdot(\kappa-\kappa')]\frac{k\cdot k'}{k^2 k'^2}\text{Im}\left[\frac{-1}{\epsilon_{k,\omega}}\right] \, .$$
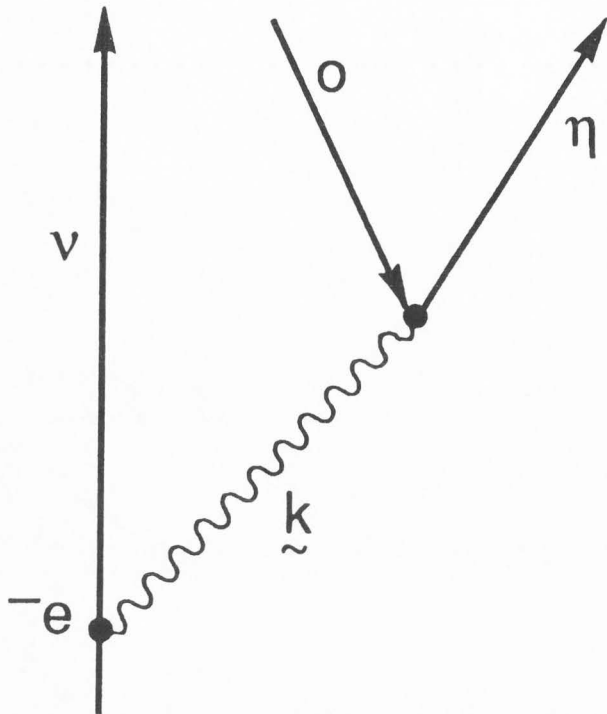
Figure 5. A Feynman diagram representing the process of creation of a virtual quasi–particle followed by the excitation of an electron–hole pair in the medium.

Then

$$\frac{d^2 \Lambda^{-1}_{ET}}{d^2 b} = \frac{e^2}{\pi^2 \hbar v^3} \int_0^\infty \omega d\omega \int_0^\infty \frac{\kappa d\kappa}{k^2} \left[\frac{\omega}{v} K_0 \left[\frac{\omega b}{v} \right] J_0(\kappa b) \right.$$

$$\left. + \kappa K_1(\kappa b) J_1 \left[\frac{\omega b}{v} \right] \right] Im \left[\frac{-1}{\epsilon_{k,\omega}} \right] \quad (28)$$

We term this the "energy transfer transform" since it agrees precisely with the formula obtained by computing the energy transferred to the medium at fixed impact parameter, using quantal dielectric theory, and then dividing the integrand in the ω variable by $\hbar \omega$. The inverse mean free path (IMFP) is found by integrating over b. The process corresponding to Eq. (28) may be represented by the Feynman diagram of Fig. 5, in which the swift electron creates an excitation in the solid which finally decays through the creation of a real electron–hole pair.

The Impact Parameter Dependence of Localized Single–Particle Transitions Induced by Unlocalized Excitations

A schematic representation of the spatial dependence of the localization of an initially unlocalized coherent excitation in an extended medium may be found. Assume that an impurity site in the medium is occupied by an electron in an orbital $\chi_o(\mathbf{r})$, situated at $\mathbf{r}$.

Let a swift electron with speed v traverse the medium at impact parameter b relative to the impurity. If the eigenenergies and wave functions of the impurity site electron are $\hbar \omega_n$ and $\chi_n(\mathbf{r}) = <\mathbf{r}|n>$ then the probability P_n that the electron is excited through virtual collective states in the medium from its ground state to the nth excited state may be written,

$$P_n = \left[\frac{e}{\pi \hbar v} \right]^2 \left| \int \frac{d^2 \kappa}{k^2} exp(i\boldsymbol{\kappa} \cdot \mathbf{b}) \right.$$

$$\times \left. \langle n | e^{i\mathbf{k} \cdot \mathbf{r}} | o \rangle \left[\frac{1}{\epsilon_{k,\omega_{no}}} \right] \right|^2 , \quad (29)$$
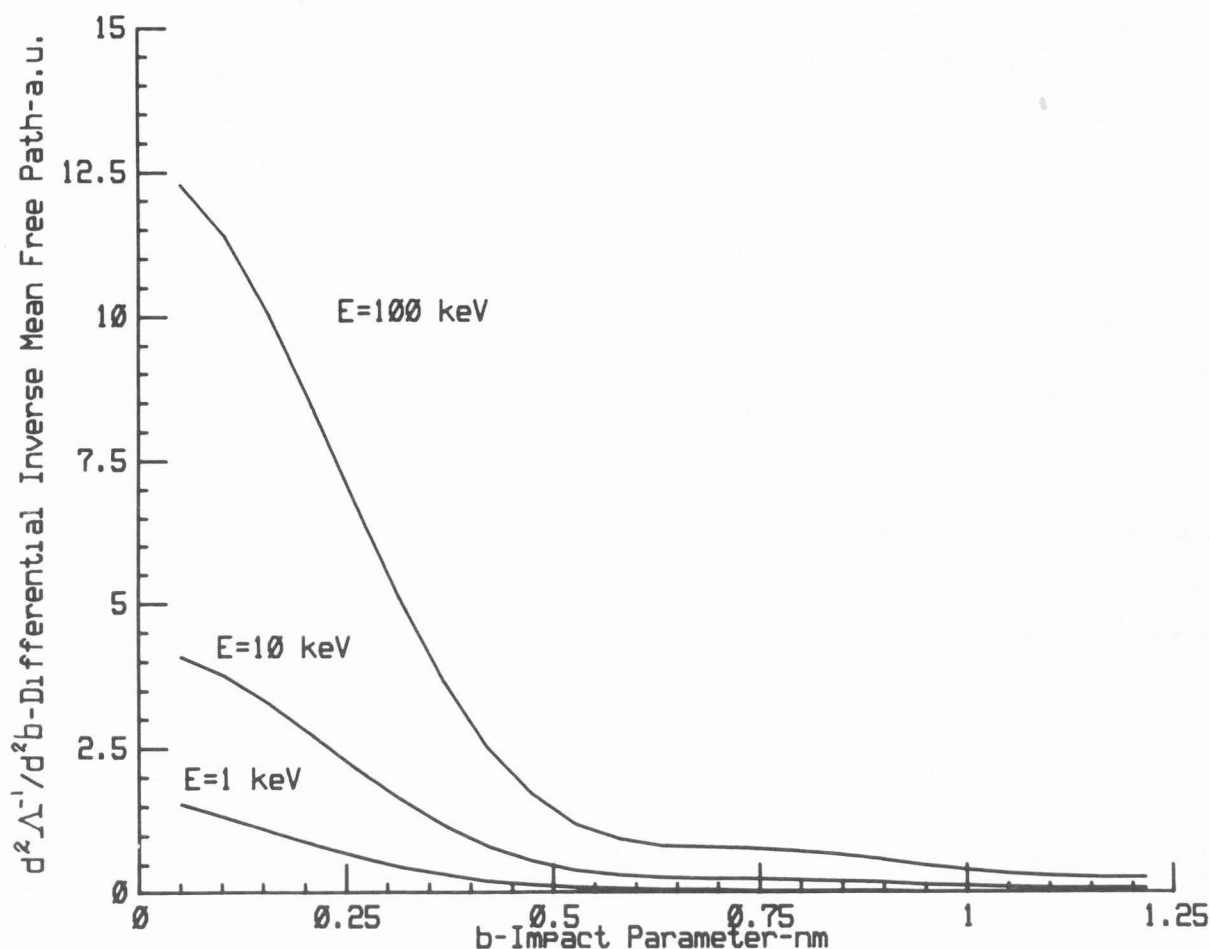
where $\omega_{no} = \omega_n - \omega_o$, $k^2 = \kappa^2 + \omega_{no}^2/v^2$, and where it is understood that the integration is to include only the region of (k,ω) space corresponding to collective states of the medium. Equation 29 is obtained by using first-order perturbation theory, assuming that the scalar electric potential at the impurity atom may be calculated from dielectric theory. In [65] this formulation is considered further.

Application of the Impact Parameter Representation

In the context of SE we use the Energy Transfer Transform of Eq. 28 above to obtain the distribution in impact parameter of energy deposition in the conduction band of aluminum metal. We take the plasmon–pole dielectric function of the electron gas to represent the response of the medium [65]. Figure 6 shows the IPR distribution calculated from Eq. 28 for three different electron energies. To obtain these results we have integrated Eq. 28 over κ by numerical quadrature. The somewhat surprising result is that each of the curves decreases as b increases, going asymptotically as $exp(-2\omega_p b/v)$ when b $\longrightarrow \infty$. It turns out that for each of these primary energies the mean value of b, averaged over these distributions is less than 1 nm. For emphasis in plotting the calculated DIMFP values have been multiplied by $2\pi \hbar v^3/e^2 \omega_p^2$. The small fluctuations in these curves correspond to quantal effects in the plasmon field. These results turn out to be quite insensitive to the damping constant assumed in the dielectric model. Note that propagation and decay of the plasmon are described in detail in this treatment. It appears that the narrow spatial resolution of these IPR distributions is due to the presence of relatively large momentum components in the interaction spectrum of the swift electron and the electron gas.

Summary and Conclusions

A self–energy formulation of the interaction between a STEM electron and a general condensed matter target has been given. It is shown that if most of the inelastically scattered electrons are collected by the energy-loss spectrometer, a classical treatment of the interaction process is valid, even in very inhomogeneous situations, provided the results are averaged over a bundle of trajectories corresponding to the size of the focused probe. Classical dielectric theory of target excitation for various geometries is discussed. The problem of spatial resolution in SEM when low–loss valence excitations occur is addressed by introducing an

Figure 6. A plot of $d^2\Lambda^{-1}/d^2b$, the inverse mean free path differential in impact parameter b, versus b, for three different electron energies, calculated from Eq. 28. For convenience in plotting, the curves have been scaled by multiplying the results from Eq. 28 by the factor $2\pi\hbar v^3/e^2\omega_p^2$, where v is the electron speed.

impact parameter representation of the interaction cross section. It is shown, using a reasonable model of the DIMFP, that the experimental SE data showing high spatial resolution may be accounted for by the presence of large momentum components in the electron–valence band interaction spectrum.

Acknowledgements

References

[1]   Ruthemann G. (1941). Diskrete energieverluste schneller elektronen in festkorpern. Naturwiss.29,648–649
[2]   Ruthemann G. (1948). Elektronenbremsung an Rontgenniveaus. Ann. Physik (6 folge) 2, 135–146
[3] Pines D. (1953). A collective description of electron interactions: IV. Electron interaction in metals. Phys. Rev. 92, 626–636

[4] Ritchie RH. (1957). Plasma losses by fast electrons in thin films. Phys. Rev. 106, 874–881
[5] Powell CJ, Swan JB. (1959). Origin of characteristic electron energy losses in Al. Phys. Rev. 115, 869–875
[6]   Raether H. (1980).   Excitation of plasmons and interband transitions by electrons. Springer Tracts, Vol. 88, Springer–Verlag, New York.
[7]   Ritchie RH, Howie A. (1988). Inelastic scattering probabilities in scanning transmission electron microscopy. Phil. Mag. 58, 753–767
[8]   Feynman RP. (1949). Space–time approach to quantum electrodynamics. Phys. Rev. 76, 769–789
[9]   Hedin L, Lundqvist S. (1969). Effects of electron–electron and electron–phonon interaction on the one–electron states of solids. Solid State Phys. 23, 1–181
[10]   Inkson JC. (1973). The effective exchange and correlation potential of metal surfaces. J. Phys. F3, 2143–2156
[11] Manson JR, Ritchie RH. (1981). Self–energy of a charge near a surface. Phys. Rev. B24, 4867–4870
[12]   Zheng X, Ritchie RH, Manson JR. (1989). High–order corrections to the image potential. Phys.

Rev. B39, 13510–13513.

[13] Echenique PM, Bausells J, Rivacoba A. (1987). Energy–loss probability in electron microscopy. Phys. Rev. B35, 1521–1524

[14] Kohl H. (1983). Image formation by inelastically scattered electrons: image of a surface plasmon. Ultramicroscopy 11, 53–66

[15] Kohl H, Rose H. (1985). Theory of image formation by inelastically scattered electrons in the electron microscope. Adv. Electr. Elect. Phys. 65, 173–227

[16] Schultz TD. (1964). Quantum theory and the many–body problem. Gordon and Breach, New York, 1–106

[17] Inkson JC. (1984). Many–body theory of solids. Plenum Press, New York, 135–182

[18] Ritchie RH, Marusak AL. (1966). The surface plasmon dispersion relation for an electron gas. Surf. Sci. 4, 234–240

[19] Ritchie RH, Wilems RE. (1969). Photon–plasmon interaction in a nonuniform electron gas. Phys. Rev. 178, 372–381

[20] Echenique PM, Ritchie RH, Barberan N, Inkson JC. Semiclassical image potential at a solid surface. Phys. Rev. B23, 6486–6493

[21] Echenique PM, Pendry JB. (1976). Absorption profile at surfaces. J. Phys. C8, 2936–2942

[22] Ritchie RH, Manson JR. (1987). Long–range interactions between probes, particles and surfaces. Int. J. Quant. Chem.: Quant. Chem. Symp. 21, 363–375, Ed. P. Löwdin, Wiley Interscience

[23] Warmack RJ, Becker RS, Anderson VE, Ritchie RH, Chu YT, Little J, Ferrell TL. (1984). Surface–plasmon excitation during aloof scattering of low–energy electrons in micropores in a thin metal foil. Phys. Rev. B29, 4375–4381

[24] Howie A. (1983). Surface reactions and excitation. Ultramicrosc. 11, 141–148

[25] Marks LD. (1982). Observation of the image force for fast electrons near an MgO surface. Solid State Comm. 43, 727–729

[26] Cowley JM. (1982). Surface energies and structure of small crystals. Surf. Sci. 114, 587–606

[27] Howie A, Milne RH (1984). Electron energy loss spectra and reflection images from surfaces. J. Microsc. 136, 279–285

[28] Garcia-Molina R, Gras-Marti A, Howie A, Ritchie RH. (1985). Retardation effects in the interaction of charged particle beams with bounded condensed media. J. Phys. C18, 5335–5345

[29] Echenique PM. (1985). Dispersion effects in the excitation of interfaces by fast electron beams. Phil. Mag. 52,L9–L13

[30] Milne RH, Echenique PM. (1985). The probability of MgO surface excitations with fast electrons. Solid State Comm. 55, 909–910

[31] Walls MG, (1988) Electron energy loss spectropscopy of surfaces and interfaces, PhD thesis, University of Cambridge, UK

[32] Fan Cheng–gao, Howie A, Walsh CA, Yuan Jun. (1989). Localised valence energy loss spectroscopy in the scanning transmission electron microscope. Solid State Phenom. (Leichenstein)), B5, 15–30

[33] Walls MG, Howie A. (1989) Dielectric theory of localised valence energy loss spectroscopy. Ultramicrosc. 28, 40–43

[34] Howie A, Milne RH. (1985). Excitations at interfaces and small particles. Ultramicrosc. 18, 427–434

[35] Ferrell TL, Echenique PM. (1985). Generation of surface excitations on dielectric spheres by an external electron beam. Phys. Rev. Lett. 55, 1526–1529

[36] Echenique PM, Howie A, Wheatley DJ. (1987). Excitation of dielectric spheres by external electron beams. Phil. Mag. B56, 225–349

[37] Acheche A, Colliex C, Kohl H, Nourtier A, Trebbia P. (1986) Theoretical and experimental study of plasmon excitation in small metallic spheres. Ultramicrosc. 20,99–106

[38] Wang ZL, Cowley JM. (1987) Surface plasmon excitation for supported metal particles. Ultramicrosc. 21, 77–94

[39] Wang ZL, Cowley JM. (1987) Excitation of the supported metal particle surface plasmon with an external electron beam. Ultramicrosc. 21, 335–365

[40] Batson PE. (1982). Surface plasmon coupling in clusters of small spheres. Phys. Rev. Lett. 49, 936–940;

[41] Batson PE. (1985) Inelastic scattering of fast electrons in clusters of small spheres. Surf. Sci. 156, 720–737

[42] Illman BL, Anderson VE, Warmack RJ, Ferrell TL. (1988) Spectrum of surface–mode contributions to the differential energy–loss probability for electrons passing by a spheroid. Phys. Rev. B38, 3045–3049

[43] Garcia–Molina R, Gras–Marti A, Ritchie RH. (1985) Excitation of Edge Modes in the interaction of electron beams with dielectric wedges. Phys. Rev. B31, 121–126

[44] Boardman AD, Garcia–Molina R, Gras–Marti A, Louis E. (1985) Electrostatic edge modes of a hyperbolic dielectric wedge: analytical solution. Phys. Rev. B32, 162–166

[45] Chu YT, Warmack RJ, Ritchie RH, Little JW, Becker RS, Ferrell TL. (1984). Contribution of the surface plasmon to energy losses by electrons in a cylindrical channel. Particle Accelerators 16, 13–17

[46] De Zutter D, De Vleeschauwer D. (1986). Radiation from and forces acting on a point charge moving through a cylindrical hole in a conducting medium. J. Appl. Phys. 59, 4146–4150

[47] Zabala N, Rivacoba A, Echenique PM. (1988). Energy loss of electrons traveling through cylindrical holes. Surf. Sci. 209, 465–480.

[48] Cheng SC. (1987). Localization distance of plasmons excited by high–energy electrons. Ultramicrosc. 21, 291–292

[49] Scheinfein M, Muray A, Isaacson M. (1985). Electron energy loss spectroscopy across a metal–insulator interface at sub–nanometer spatial resolution. Ultramicrosc. 16, 233–240

[50] Batson PE, Kavanagh KL, Woodall JM, Mayer JW. (1986). Electron–energy–loss scattering near a single misfit location in a dielectric medium of randomly distributed metal particles. Phys. Rev. Lett. 57, 2729–2732

[51] Bleloch AL, Howie A, Milne RH, Walls MG. (1989) Elastic and inelastic scattering effects in reflection electron microscopy. Ultramicrosc. 29, 175–182

[52] Imeson D, Milne RH, Berger SD, McMullan D (1985) Secondary electron detection in the scanning transmission electron microscope. Ultramicroscopy 17, 243–250

[53] Chung MS, Everhart TE. (1977). Role of plasmon decay in secondary electron emission in the nearly–free–electron metals. Application to aluminum. Phys. Rev. B15, 4699–4714

[54] Rosler M, Brauer W. (1981) Theory of secondary el4ctron emission I. General theory for nearly–free–electron metals. Phys. Stat. Sol. b104, 161–175

[55] Rosler M, Brauer W. (1981). Theory of secondary electron emission. II. Application to Aluminum. Phys.

Stat. Sol. b104, 575–587

[56] Rosler M, Brauer W. (1988) Theory of electron emission from solids by proton and electron bombardment. Phys. Stat. Sol. b148, 213–226

[57] Luo S, Joy DC. (1988). Monte Carlo calculations of secondary electron emission. Scanning Microsc. 2, 1901–1915

[58] Ritchie RH, Brandt W. (1975) Primary processes and track effects on irradiated media. Radiation Research; Biomedical, Physical and Chemical perspectives, Academic Press, New York, 315–320.

[59] Ritchie RH. (1975) Theoretical aspects of channeling, in The Channeling of Particles, Proceedings of a conference at the Institut National des Sciences et Techniques Nucleaires, Gif–sur–Yvette, France, 47–59, A. Sarazin, Ed. CEA, Service de Documentation, Saclay

[60] Bohr N. (1913). On the decrease of velocity of swiftly moving electrified particles in passing through matter. Phil. Mag. (6) 25, 10–31

[61] Williams EJ. (1945). Space–time concepts in collision problems. Rev. Mod. Phys. 17, 217–245

[62] Neufeld J. (1953). Energy losses of charged particles of intermediate energy. Proc. Phys. Soc. (London) A66, 489–596

[63] Fano U. (1960). Collective effects in absorption of energy from ionizing radiation. Comparative Effects of Radiation. Burton E, Kirby–Smith J, Magee J, Eds. John Wiley and Sons, New York, 14–21

[64] Chang NP, Raman K. (1969). Impact parameter representation and the coordinate-space description of a scattering amplitude. Phys. Rev. 181, 2048–2055

[65] Ritchie RH, Hamm RN, Turner JE, Wright HA, Ashley JC, Basbas GJ. (1989). Physical aspects of charged particle track structure. Nuclear Tracks and Radiation Measurements, in press

[66] Mermin ND. (1970). Lindhard dielectric function in the relaxation–time approximation. Phys. Rev. B1, 2362–2363

Discussion with Reviewers

P. Schattschneider: The Feynman diagram Fig. 5 to which you refer after Eq. 28 shows a process where a particular momentum $\hbar k$ is transferred to an electron–hole pair excitation via a plasmon. How does this relate to Eq. 28 where a position variable b occurs and the momentum is integrated out?

Authors: This diagram illustrates the elemental virtual processes that contribute to the IMFP. To obtain the IMFP of Eq. 28 or Eq. 29, it is necessary to transform variables from momentum transfer to impact parameter.

P. Schattschneider: In the derivation of Eq. 18 you assume a geometry as sketched in Fig. 3. The impact parameter b has a precise meaning there. The procedure leading to the Chang–Raman transform follows closely the derivation of the density autocorrelation function in a homogeneous medium given by Van Hove. Consequently, I would expect Expression 28 to contain information on the (radial) distribution of the coherently induced charge at distance b from a randomly selected point in the homogeneous medium. From that, it seems to me that you use the work "impact parameter" in two different ways: the "b" in the first part of the paper is a distance between target and probe, whereas "b" in Eq. 28 is a distance between points in the target which oscillate coherently. What, then, is the meaning of the "impact parameter" b in Eq. 28, and is it different from that leading to Eq. 18?

Authors: The derivation leading to the Chang–Raman transform of Eq. 27 does contain information about the radial distribution of coherently induced excitations at distance b from the track of the particle. However, Eq. 28, although obtained using a different transformation of variables, agrees exactly with the result found by using dielectric theory to calculate the energy transferred to the medium. This is indicated following Eq. 28. Thus the physical interpretation of Eq. 28 is straightforward and corresponds to the concept of an impact parameter not very different from that used in Eq. 28.

P. Schattschneider: Why is the Energy–Transfer transform preferable to the Chang–Raman transform?

Authors: For the reason given in the last answer and because of the fact that the Chang–Raman transform seems to produce indeterminate results when narrow resonances occur in the response function of the medium [61].

P. Schattschneider: Is it meaningful to relate some momentum transfer, say $\hbar/b$ from a simple reciprocal space argument, to the energy–transfer transform in order to access it in diffraction mode EELS? Or else can you describe an experimental setup with which the energy–transfer transform is accessible directly? Can you possibly do it in a macroscopically homogeneous specimen?

Authors: The answers to these questions are not clear to us.

P. Schattschneider: You state that the oscillations in Fig. 6 are of quantal nature. In a similar result, given in Ref. [61], those oscillations are missing. Can you comment on that?

Authors: Such oscillations are easy to see in Fig. 12 of Reference [61] but are more difficult to perceive in Fig. 11 because of their small amplitude.

K. Krishnan: The plasmon excitation is, in principle, a delocalized process. Could you please clarify or explain your definition of an impact parameter for measurements of this phenomenon? In addition, there is a lot of excitement generated by the development of secondary electron detection with polarization analysis. A high current density source is used and spatial resolutions of 10 nm are claimed. Could you comment on the applicability of your impact parameters in defining spatial resolution in the context of measurements of such delocalized emissions?

Authors: See the discussion above. Also, our interpretation of the results we show in Fig. 6 is that the probability of SE due to the generation of an electron–hole pair by a plasmon at impact parameter b from the point at which a fast electron impinges on a solid should be narrowly concentrated in a region $\lesssim 1$nm from that point for energies of interest in STEM. We feel that these results should be applicable to SE detection with polarization analysis.

J. Schou: Does your treatment show that a bulk plasmon in aluminum (and other metals) is very likely to decay within 0.25 nm from the point of impact of the primary electron?

Authors: As indicated in the discussion of Fig. 6 following Eq. 29, for the primary energies studied, decay is expected to occur with a mean value of b $\lesssim 1$nm.

J. Schou: What is your opinion of the feasibility of the previous treatments by Rösler and Brauer and of Chung and Everhart on the plasmon creation and decay in secondary electron emission? In which respects do their treatment differ from yours?

Authors: We cannot comment on the details of these treatments since the calculations are quite intricate. However, their models of plasmon generation and decay seem quite reasonable. Of course, we do not attempt to include the effect of electron transport and cascade in our work. Rather, our results refer to the spatial distribution of decay of quasiparticles such as plasmons into first generation electron—hole pairs. Since the energies of the electrons generated in these decays are ~10 eV, the transport and cascade of such electrons should occur over very small distances (<1nm).

P. Nordlander: Why is the plasmon coupling depending on the impact parameter b? Plasmons are a collective motion of the conduction electrons and as such delocalized along the surface. I would therefore not expect any b dependence.

Authors: We do not assume that plasmon coupling with SE per se depends upon b. However, we do study the probability of deexcitation of the collective mode field as a function of distance from the point of creation of the mode.

C. Humphreys: The classical impact parameter model, and the well—known uncertainty principle argument, yield that the localization of an inelastic scattering event is a function of the incident electron energy. Your new theorem suggests not only that the localization is substantially greater than previously thought, but also it appears to be largely independent of the incident electron energy. Is my interpretation of your theorem correct? Do you have a qualitative explanation for why your new theorem yields a greater localization than previous theories?

Authors: As indicated above, the large b—dependence of the DIMFP in impact parameter space does indeed vary somewhat with the velocity of the incident electron. However, it appears that large momentum components in the electron—plasmon spectrum should give rise to a distribution of SE from the decay of the plasmon that are narrowly concentrated about the entry point of a fast electron.

L. W. Hobbs: In wide—gap insulators, bound electron—hole excitons states are spatially highly localized. Is there anything you know of which precludes decay of spatially—extensive valence plasmons into two (or more) widely—spatially separated single electron—hole bound states? This question is of some interest to those who are concerned with radiolytic damage processes in solids in which the efficiency of producing single exciton states from other, more probable excitations is especially relevant.

Authors: In principle the decay of collective states into two or more electron—hole pairs should occur. However, one suspects that the probability of such processes may be small compared with the probability of decay into a single electron—hole pair. For example, theoretical [J. C. Ashley and R. H. Ritchie, *Phys. Status Solidi* 38, 425 (1970)] and experimental [see, e.g., P. Schattschneider et al., *Phys. Rev. Letters* 59, 724 (1987)] studies of the process in which a single plasmon decays into two plasmons in metallic systems shows that this occurs with small probability relative to the single decay channel probability. Although not directly relevant to the question posed, the expressions for the rates of these compound processes have some similarities.